Nanoscale

PAPER

View Article Online
View Journal | View Issue

Check for updates

Cite this: *Nanoscale*, 2024, **16**, 18389

Rational (supra)molecular design and catalytic activity of cage-like Cu_4-based phenylsilsesquioxanes†

Anna Y. Zueva,[a,b] Alexey N. Bilyachenko, *[a,b] Victor N. Khrustalev, [b,c] Lidia S. Shul'pina,[a] Nikolay S. Ikonnikov,[a] Pavel V. Dorovatovskii, [d] Elena S. Shubina, [a] Karim Ragimov,[e] Nikolai N. Lobanov[b] and Di Sun *[f]

Received 22nd May 2024,
Accepted 22nd August 2024

DOI: 10.1039/d4nr02173h

rsc.li/nanoscale

Published on 03 2024. Downloaded on 14.08.25 19:54:21.

An extended (*i.e.*, 19 distinct species) family of cage-like Cu_4-phenylsilsesquioxanes allowed us to accentuate the general regularities behind their structural organization. Influencing factors, namely the (i) size of external alkali metal ions (from Li to Cs) and (ii) nature of bridging linkers (including the smallest possible ones, like a water molecule) on the self-assembly/supramolecular assembly of such Cu_4-building blocks have been thoroughly explored. A Cu_4K_4-based complex has been evaluated as a precatalyst in the oxidation of alkanes (cyclohexane, *n*-heptane, methylcyclohexane) and alcohols. The experimental evidence that radical species participate in the oxidation of alkanes is provided.

Introduction

The ability of metallocomplexes based on silsesquioxane $[RSiO_{1.5}]_n$ ligand matrices to form extraordinary cage molecular geometries (cage-like metallosilsesquioxanes CLMSs) is well documented.[1] Enormous variety of compositions and structures of CLMSs endow them with an impressive list of properties and applications. CLMSs may be applied for the design of molecular magnets[2] (including examples of spin glass[3] and single molecule magnets[4]). Recent results have pointed out the rich photophysics of CLMSs,[5] with the lanthanide-based family of such complexes being especially attractive, holding promise for energy transfer,[6] remote temperature sensing,[7] or thin-film optoelectronics.[8] For prospective materials, CLMSs were applied for the creation of intumescent objects,[9] anodes,[10] functional coordination polymers,[11] calcined derivatives,[12] and fungicides.[13] Catalytic properties of CLMSs attracted considerable attention,[14] including recent results on the Chan–Lam coupling,[15] formation of bio-inspired ethers,[16] oxidation of volatile organic compounds,[17] and deacetalization/deketalization-Knoevenagel reactions.[18] Further design of CLMSs as potential catalysts towards reactions of high demand, especially functionalization of hydrocarbons,[19] remains an actual scientific task. Regarding the synthetic approaches to CLMSs, two main tactics exist. The first one indicates the involvement of the prebuilt silsesquioxane ligands (mostly Si_7-based cubane triol).[1b,e,g,2d,6,12b,16,18] Alternative approach relies on the *in situ* formation of silsesquioxane ligands starting from the simple reactant, *e.g.*, $PhSi(OMe)_3$.[1k,2b,c,3–5,7,8] This latter approach (self-assembly of ligand just prior self-assembly of metallocomplex) provides considerable flexibility of CLMS structures. In this paper, we discuss the self-assembly features of CLMSs with Cu_4 derivatives as an example. A record-holding large number of tightly related CLMSs (19 individual island-like complexes or coordination polymers) were examined in terms of the role played by (i) solvating ligands (linkers) and (ii) external ions (of alkali metal) in the molecular/supramolecular structure formation. We report on the catalytic properties of a representative Cu_4K_4-CLMS in the peroxide oxidation of alkanes with hydrogen peroxide and alcohols with *tert*-butylhydroperoxide.

Results and discussion

Synthesis and structure

A specific feature of heterometallic CLMSs simultaneously bearing transition and alkali metal ions indicates that transition metal ions are located inside the cage while alkali metal

[a]*A.N. Nesmeyanov Institute of Organoelement Compounds, Russian Academy of Sciences, Vavilov Str. 28, 119991 Moscow, Russia. E-mail: bilyachenko@ineos.ac.ru*
[b]*Peoples' Friendship University of Russia (RUDN University), Miklukho-Maklay Str. 6, 117198 Moscow, Russia*
[c]*Zelinsky Institute of Organic Chemistry, Russian Academy of Sciences (RAS), Leninsky Prospect 47, 119991 Moscow, Russia*
[d]*National Research Center "Kurchatov Institute", Akademika Kurchatova pl. 1, 123182 Moscow, Russia*
[e]*Baku State University, Z. Xalilov Str. 23, Az 1148 Baku, Azerbaijan*
[f]*Department of Chemistry and Chemical Engineering, Shandong University, Shanda South Road 27, 250100 Jinan, China. E-mail: dsun@sdu.edu.cn*

† Electronic supplementary information (ESI) available. CCDC 2355320-2355338. For ESI and crystallographic data in CIF or other electronic format see DOI: **https://doi.org/10.1039/d4nr02173h**

Published on 03 2024. Downloaded on 14.08.25 19:54:21.

ions are located outside the cage.[1f,h] Due to these external positions, several examples of CLMS' coordination polymers assembled *via* alkali metal-enabled contacts have been designed.[1k] These coordination polymers (Chart 1) reveal either crown ether contacts *via* alkali metal ions leading to (i) porous MOF (Cu_6K_2-compound[20]) or (ii) 1D extended (Cu_8Cs_2-compound[21]) structures.

Below, we present our investigation of the applicability of the alkali metal ions (Li–Na–K–Rb–Cs) for the purposeful aggregation of CLMSs' coordination polymers. As the transition metal sites, copper(II) ions have been chosen. To obtain the corresponding heterometallic compounds, a well-established scheme, including alkaline hydrolysis of $PhSi(OMe)_3$ with MOH[22] was applied. In the second stage, intermediate $[PhSi(O)OM]_n$ phenylsiloxanolate species formed *in situ* interact with a source of copper centres ($CuCl_2$). Due to the lowest ionic radii among alkali metals, a high "inter-cage efficacy" in terms of CLMS assembly is hardly expected for lithium. Indeed, the first run of this synthetic scheme (Fig. 1, top), with LiOH picked as a starting alkali reagent, afforded an island-like compound $\{[(Ph_{12}Si_{12}O_{24})Li_4Cu_4(EtOH)_8]\}\cdot\{[(Ph_{12}Si_{12}O_{24})Li_4Cu_4(EtOH)_6(H_2O)]\}$ (**1**, 70% yield). Compound **1** (Fig. 1, bottom) adopts a cage-like structural type, with a large twelve-membered cyclic silsesquioxane ligand embracing the central copper-containing core, while lithium ions are located in external positions. In summary, metal centers form two orthogonal linear fragments with the Li···Cu···Cu···Li composition (Fig. 2). Two independent cage components in **1** are structurally very similar to each other. In particular, this could be concluded from a comparison of distances between opposite lithium ions in the two independent cages (they are equal to

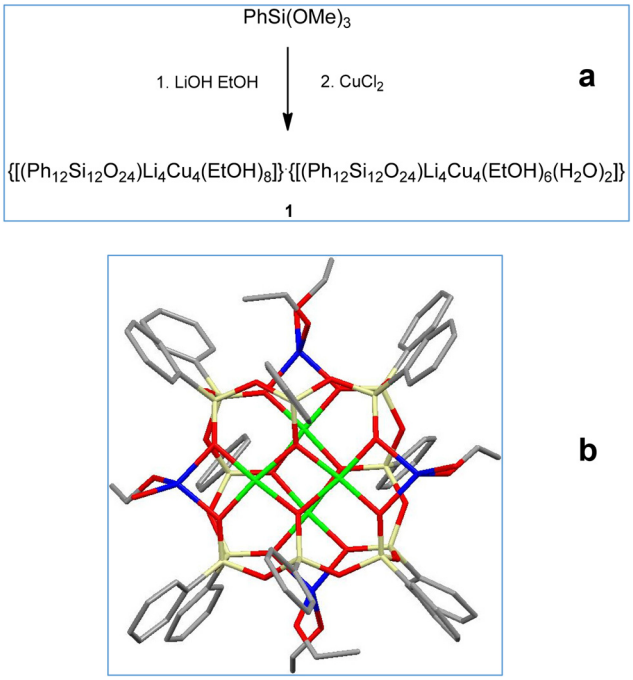

Fig. 1 (a) A general method for the synthesis of Cu_4Li_4-phenylsilsesquioxane **1**. (b) The molecular structure of **1**. Color code: green Cu; yellow Si; red O; grey C; blue Li.

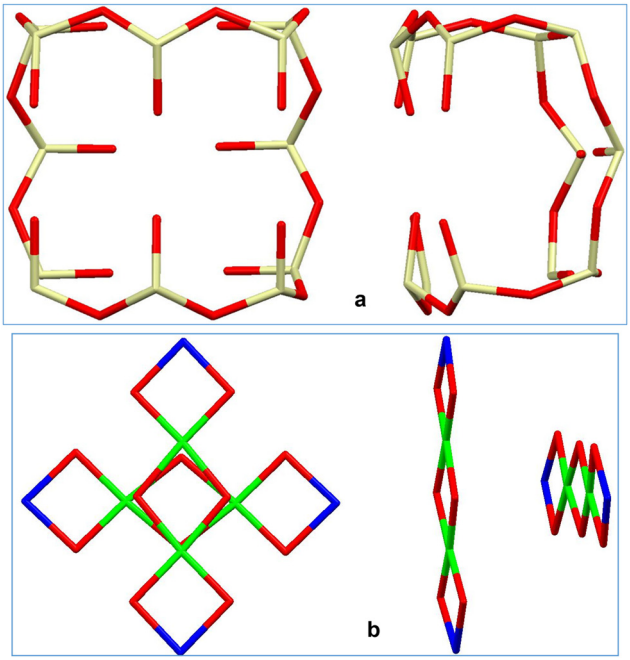

Fig. 2 (a) Two projections of twelve-membered cyclic silsesquioxane ligand in **1**. (b) Two projections of the metal-oxo cluster in **1**. Color code is the same as in Fig. 1.

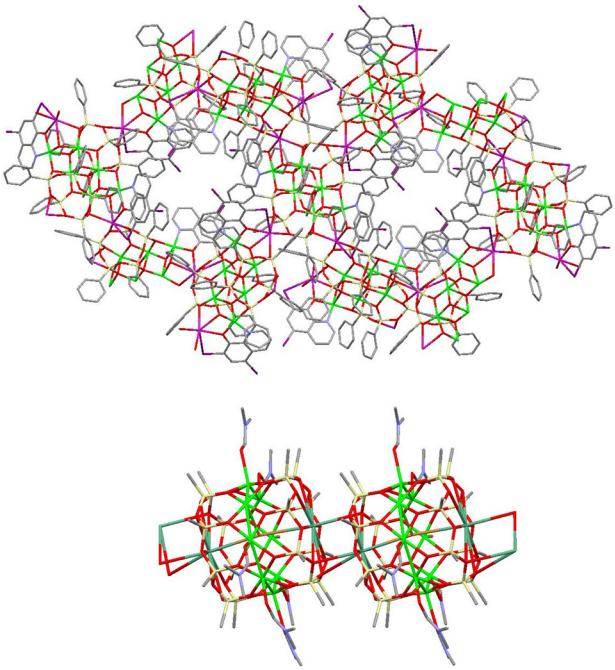

Chart 1 Examples of CLMS-based coordination polymers. Top. Fragment of a porous 3D MOF structure (Cu_6K_2-silsesquioxane[20]). Bottom. Dimeric fragment of a 1D extended structure (Cu_8Cs_2-compound[21]).

 This journal is © The Royal Society of Chemistry 2024

Published on 03 2024. Downloaded on 14.08.25 19:54:21.

8.526(16) Å and 8.515(16) Å, or 8.555(16) Å and 8.565(16) Å, respectively).

In the next stage of our study, we have shifted to sodium-based compounds (Fig. 3, top). In addition to initial conditions, when ethanol plays a dual role as a solvent for the synthesis and solvating ligand for crystallization, several other solution options have been explored. These included the replacement of ethanol by acetone or by the corresponding solvent pairs (EtOH/MeCN, EtOH/acetone, EtOH/diethyl ether). As a result, corresponding compounds, namely: $[(Ph_{12}Si_{12}O_{24})Na_4Cu_4(EtOH)_6]\cdot 2EtOH$ (**2**, 73% yield), $[(Ph_{12}Si_{12}O_{24})Na_4Cu_4(Me_2CO)_8]$ (**3**, 69% yield), $\{(Ph_{12}Si_{12}O_{24})Na_4Cu_4(EtOH)_{5,2}(MeCN)_2(H_2O)_{0,8}\}\cdot\{(Ph_{12}Si_{12}O_{24})Na_4Cu_4(EtOH)_4(MeCN)_2(H_2O)_2\}$ (**4**, 58% yield) $[(Ph_{12}Si_{12}O_{24})Na_4Cu_4(Me_2CO)_4(EtOH)_4]$ (**5**, 68% yield), $[(Ph_{12}Si_{12}O_{24})Na_4Cu_4(Et_2O)_4(EtOH)_2]$ (**6**, 62% yield; **6a**, 60% yield) have been successfully isolated. All compounds **2–6** (Fig. 3, bottom) belong to the structural type **1**, with a Si_{12}-silsesquioxane ligand and the Cu_4Na_4 core. To our surprise, we noticed that the replacement of lithium ions in **1** by sodium ions in **2–6** caused a significant structural distortion. Namely, one could observe a bent Na···Cu···Cu···Na fragment in **3**, **5–6a**

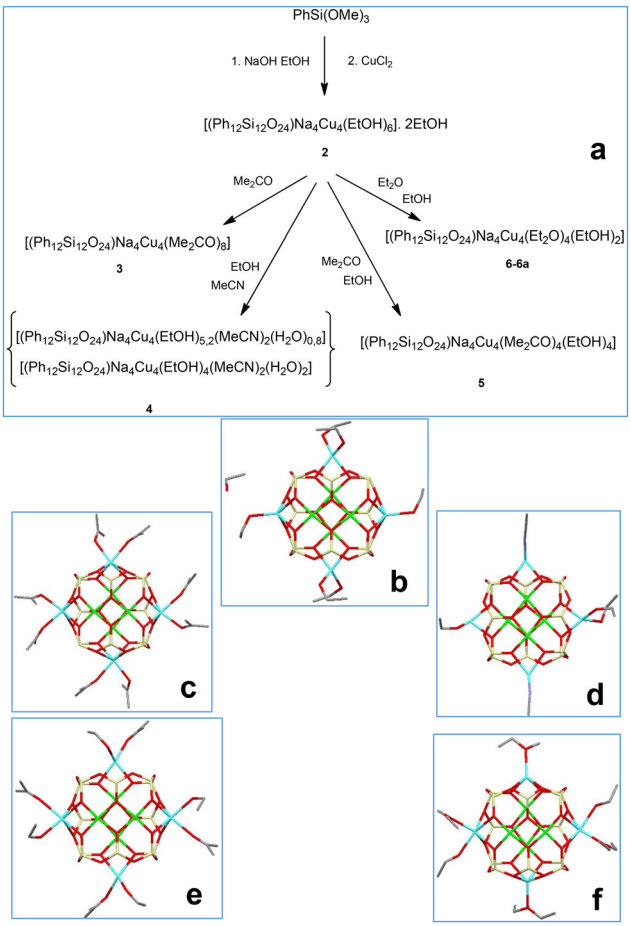

Fig. 3 (a) A general method for the synthesis of Cu_4Na_4-phenylsilsesquioxanes **2–6**. (b–f) The molecular structures of **2–6**. Color code is the same as for Fig. 1, but cyan Na.

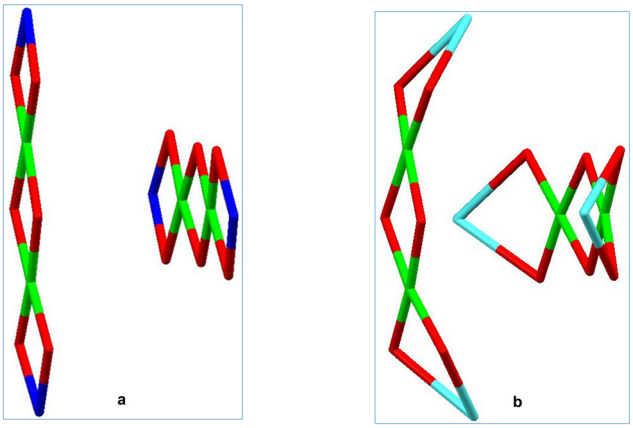

Fig. 4 Comparison of linear (a) and bent (b) metal-oxo clusters in **1** and **3**, **5–6a**, respectively. Color code is the same as for Fig. 1 and 3.

(Fig. 4) instead of a linear Li···Cu···Cu···Li fragment in **1**. Only complex **4** adopts a linear principle similar to **1**. Noteworthily, very recently, we have already reported on a specific role played by the lithium ion (along the Li–Na–K series) on the self-assembly of Fe(III)-silsesquioxane/acetylacetonate complexes,[19d] and this "Li-feature" is further confirmed here. Another influential aspect altering the structure of cages **2–6** is the nature of the solvating ligands, which could be illustrated by the variation of distances between opposite sodium centers. Namely, Na···Na distances are equal to 8.420(3) and 9.241(4) Å (for **2**), 9.246(8) and 8.704(9) Å (for **5**), 8.857(4) and 8.396(3) Å (for **6**), 8.851(4) and 8.407(4) Å (for **6a**). Complexes **6** and **6a** represent different conformers and are distinguished only by the conformations of ether ligands bound to sodium ions. Note that acetone-solvated cage **3** possesses the symmetrical structure (both Na···Na distances are equal to 8.600(4) Å), as well as complex **4** with the Na···Na distances of 9.201(9)/9.218(8) and 9.218(8)/9.213(8) Å (for the two crystallographically independent cages) without such variations.

We suggested that the formation of coordination polymers in the case of all complexes **2–6** was not realized due to screening effects of solvates at sodium centres. To force the formation of desired extended polymeric structures, it would be logical to try to use water since water molecules are characterized by minimum steric limitations among any widely used solvents. In line with these thoughts, we performed the "CuNa-silsesquioxane **2**-targeted" syntheses but in the presence of an additional amount of water (Fig. 5, top). As a result, the corresponding water-containing complexes have been isolated, namely, $[(Ph_{12}Si_{12}O_{24})Na_4Cu_4(EtOH)_{1,5}(H_2O)_5]\cdot(EtOH)$ (**7**, 52% yield) and $[(Ph_{12}Si_{12}O_{24})Na_4Cu_4(H_2O)_4(EtOH)_{3,5}]\cdot\frac{1}{2}(EtOH)$ (**8**, 58% yield). Both complexes **7–8** represent a type of molecular architecture similar to compounds **2–6**. Furthermore, water molecules, due to the lower steric hindrances, give rise to extended 1D chain-like structures (Fig. 5, bottom). Variation of the number of water and ethanol solvate molecules in **6–7** causes a certain distortion in the cage structures (opposite Na···Na distances are equal to 9.343(4) and 8.703(4) Å (for **7**),

Published on 03 2024. Downloaded on 14.08.25 19:54:21.

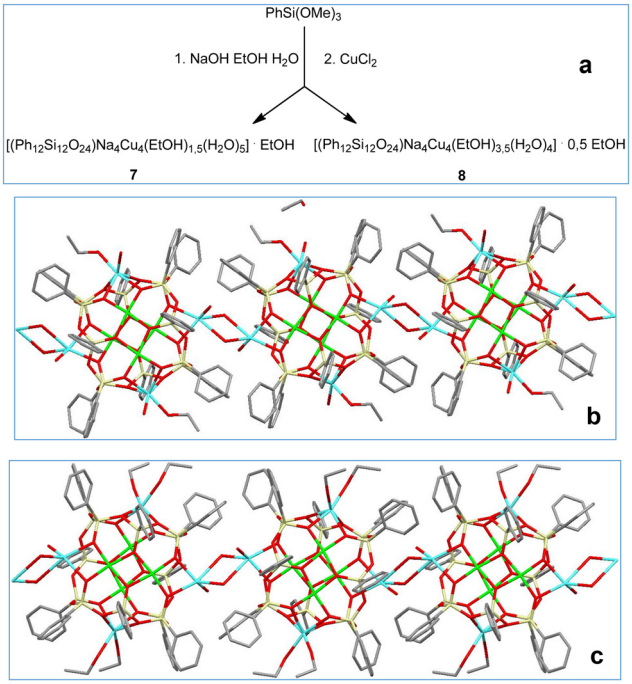

Fig. 5 (a) A general method for the synthesis of Cu_4Na_4-phenylsilsesquioxanes **7–8**. 1D supramolecular structures of **7** (b) and **8** (c).

9.320(4) and 8.732(4) Å (for **8**)). These values correspond well to those observed for **2–6**. Moreover, the formation of coordination polymer structures leads to a sharp shortening of intermolecular Na···Na contacts. For **7** and **8**, these distances are equal to 3.902(4) and 3.837(4) Å, respectively. Note that the shortest intermolecular Na···Na contact found in the case of **2–6** is equal to 5.971 Å (complex **4**).

In the next stage, we concentrated on the syntheses of potassium-containing analogs of complexes **1–8** (Fig. 6, top). A larger radius of potassium ion was expected to better promote the formation of coordination polymers than in the case of sodium-based compounds. As in the case of Na-compounds, several "solvent options" have been explored. These included original (ethanol) synthesis as well as the replacement of ethanol by solvent combinations (DMF/MeOH/EtOH, diethyl ether/MeCN/H_2O, or acetone). As a result, three compounds successfully realizing extended structures were isolated $[(Ph_{12}Si_{12}O_{24})K_4Cu_4(EtOH)_4]$ **9** (68% yield), $[(Ph_{12}Si_{12}O_{24})K_4Cu_4(DMF)_2(MeOH)_{1.25}(EtOH)_{0.5}]$ **10** (62% yield), and $[(Ph_{12}Si_{12}O_{24})K_4Cu_4(Et_2O)_2(MeCN)_2(H_2O)_2]$ **11** (60% yield) (Fig. 4, center and bottom). The molecular structures of cage complexes **9–11** perfectly correspond to those of compounds **1–7**. As in **2**, the "ethanol only-solvated" cage **9** reveals identical distances between opposite potassium centers (10.064(3) Å). A replacement of the solvent system causes significant distortion of the cage (the intra-cage K···K distances are equal to 9.857(3) and 10.190(5) Å for **10**, or 9.5664(9) and 9.8221(9) Å for **11**). At the same time, a change in the solvent systems may provoke a decrease in the dimensionality of the coordination polymer structure (2D in the cases of **9–10**, 1D in the case of

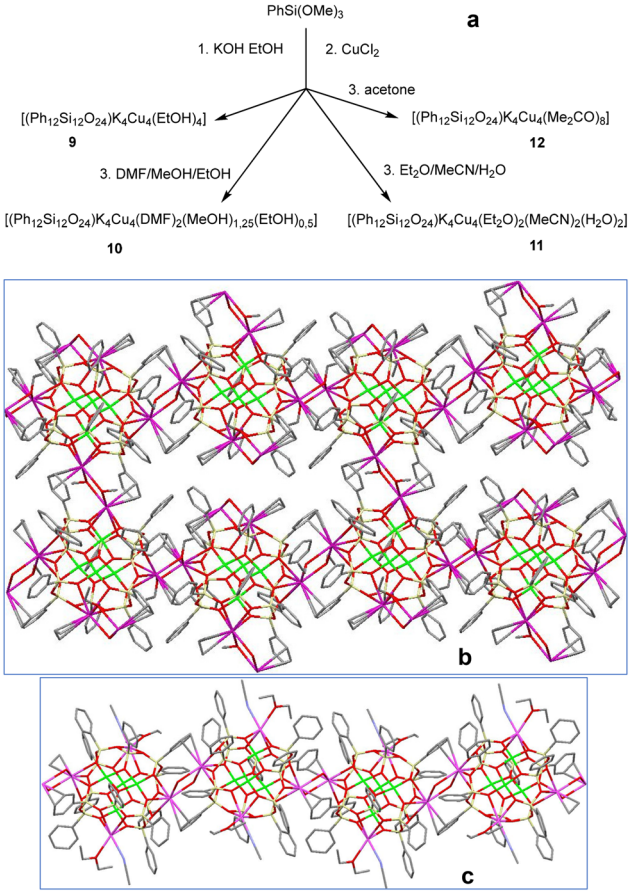

Fig. 6 (a) A general method for the synthesis of Cu_4K_4-phenylsilsesquioxanes **9–12**. (b) A simplified (flat layer) representation of 2D "stitch" supramolecular structure of **9**. (c) 1D supramolecular structure of **11**. Color code is the same as for Fig. 1, but magenta K.

11). It is intriguing that in the cases of **9** and **11**, the formation of the coordination polymer is assisted by the dual role of potassium centers. First, they form contacts with linking atoms of the solvating ligands (oxygen atom from the ethanol molecule in the case of **9** and oxygen atom from the water molecule in the case of **11**). Second, one could easily identify additional half-sandwich contacts between the potassium center from one cage and a phenyl group (at a silicon atom) from the neighboring cage. The 2D coordination polymer in **9** possesses a non-classical net structure. Indeed, one could see alternating contacts between cages in upper and lower horizontal chains (Fig. 6, center). Namely, odd cages are linked to neighboring ones, forming vertical connections. Moreover, even cages remain unlinked, forming "pore" fragments. This situation is due to different (upward *vs.* downward) directions in the growth of the coordination polymer structure from any cage in **9**, chosen as a starting one (Fig. 7). As a result, it comprises a system of interpenetrating waves (the so-called "stitch" style of 2D coordination polymers). Nevertheless, the resultant 2D coordination polymer in **9** is not porous (Fig. 6, center, shows a cross-section of the extended structure by a plane for clarity).

 This journal is © The Royal Society of Chemistry 2024

Published on 03 2024. Downloaded on 14.08.25 19:54:21.

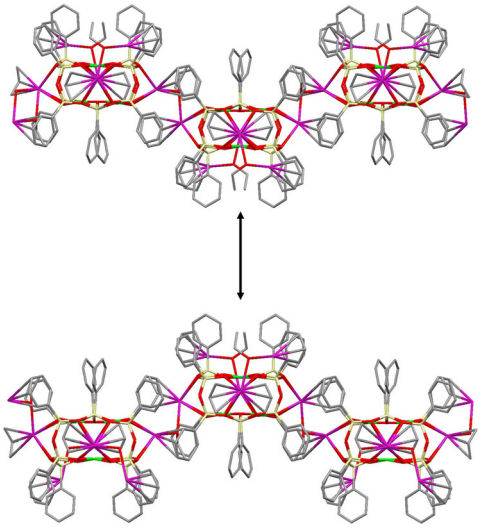

Fig. 7 Two wave-like 1D coordination polymer chains forming a 2D "stitch" structure in **9**. Central (shared by both waves) cage is shown by an arrow. Bottom chain is rotated by 90° with respect to the upper one for clarity.

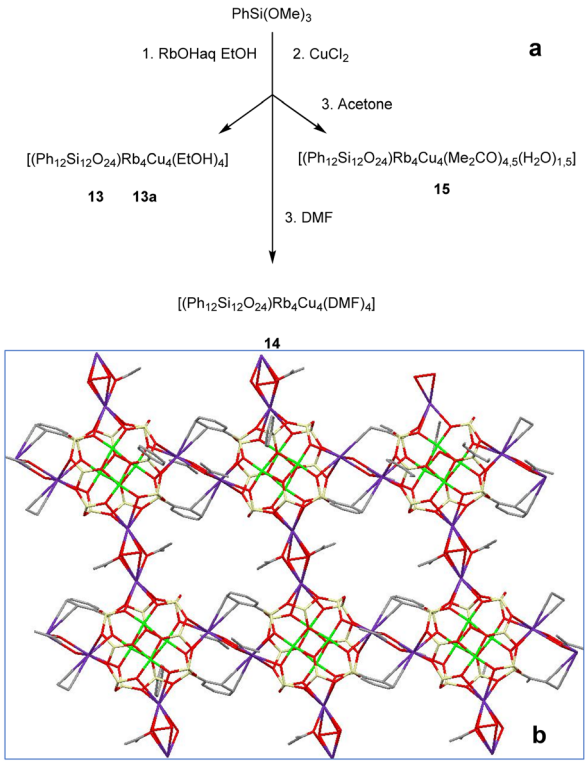

Fig. 8 (a) A general method for the synthesis of Cu_4Rb_4-phenylsilsesquioxanes **13–15**. (b) The 2D net supramolecular structure of **15**. Color code is the same as for Fig. 1, but purple Rb.

Intermolecular K···K distances for **9** are the same in all directions and equal to 4.378(3) Å.

In turn, compound **10** adopts the classical 2D net structure (Fig. S1†) *via* oxygen atoms of (i) DMF and (ii) alcohol solvates at potassium centers. Intermolecular K···K distances for **10** are equal to 4.216(3) Å (for DMF-involving contacts) and 4.124(4) Å (for alcohol-involving contacts).

The intercage connectivity of complex **11** (Fig. 6, bottom) is realized only by water-solvated potassium ions. Potassium centers coordinated by ether and acetonitrile molecules cannot form a coordination polymer due to the high steric limitations of ether-solvated molecules. The shortest intermolecular K···K distances are equal to 4.216(3) Å (for **10**) and 4.6440(10) Å (for **11**).

In line with these thoughts, solvates with even higher screening ability may totally suppress the growth of coordination polymer chains. Indeed, the fourth potassium-based complex, $[(Ph_{12}Si_{12}O_{24})\ K_4Cu_4(acetone)_8]\cdot 2(acetone)$ (**12**, 73% yield, Fig. S2†) adopts a OD island structure (the intercage K···K distances are all the same and equal to 8.678 Å). In the case of **12**, the presence of two acetone solvate molecules at each potassium center effectively prevents any supramolecular assembly.

In the next stage, we concentrated on the syntheses of rubidium-containing compounds (Fig. 8, top). Similar to complexes **7–8** and **9–11**, the resultant complexes adopt coordination polymer structures, namely, $[(Ph_{12}Si_{12}O_{24})Rb_4Cu_4(EtOH)_4]$ (**13**, 63% yield; **13a**, 60% yield), $[(Ph_{12}Si_{12}O_{24})Rb_4Cu_4(DMF)_4]$ (**14**, 67% yield), and $[(Ph_{12}Si_{12}O_{24})Rb_4Cu_4(Me_2CO)_{4.5}(H_2O)_{1.5}]$ (**15**, 71% yield). Furthermore, compounds **13–15** reveal specific distinctions. First of all, these complexes realize purely 2D supramolecular geometries. The nature of solvate molecules responsible for this exact type of supramolecular aggregation is intriguing. Namely, three compounds **13–14** belong to a "stitch" 2D structure mentioned above for compound **9**. On the other hand, compound **15** shows the classical 2D net structure (Fig. 8, bottom). The intercage connections in **13–15**, by analogy to **9–11**, are assisted by half sandwich Rb···Ph contacts. The formation of a 2D structure is finalized *via* additional contacts between rubidium ions and the corresponding linking solvates (two ethanol molecules in the case of **13–13a**; two dimethylformamide molecules in the case of **14**). In the case of **15**, one could see two different linking units: (i) with two acetone molecules and (ii) with three acetone molecules and a half water molecule. As in the case of complexes **1–12**, structural parameters of the cage components of **13–15** are sensitive to the nature of the surrounding solvate. Distances between the opposite rubidium centers in the case of DMF-complex **14** are 9.8282(16) Å and 9.9360(17) Å, but 10.0171(5) and 10.3146(5) Å for complex **15** (acetone and water act as solvate molecules therein). The intracage Rb···Rb distances are not the same even for two $EtOH_4$-solvated compounds: **13** (both distances are equal to 10.4168(5) Å) and **13a** (10.505(2) and 10.289(3) Å). This indicates that even conformational differences (the tiniest changes in the localization of ethanol molecules) may provide certain distortion of the cage geometry. The same concerns intermolecular Rb···Rb distances (equal to 4.4535(6) Å for **13**, while 4.488(2) and 4.421(3) Å for **13a**). These distances are 4.3400(5) and 4.4278(5) Å for

Published on 03 2024. Downloaded on 14.08.25 19:54:21.

15; while complex **14** reveals the most asymmetrical geometry (Fig. S3†) featuring three different distances (4.5696(13), 4.5348(9), and 4.5486(8) Å).

The final stage of our synthetic studies was aimed at isolating cesium-based compounds. The use of $CsOH_{aq}$ as a source of cesium centers (Fig. 9, top) yields two compounds, namely, $[(Ph_{12}Si_{12}O_{24})Cs_4Cu_4(EtOH)_4]$ (**16**, 72% yield) and $[(Ph_{12}Si_{12}O_{24})Cs_4Cu_4(EtOH)_{4.75}]\cdot EtOH$ (**17**, 61% yield). A difference in the number of coordinated and solvated ethanol molecules causes little differences in the resultant cage structures. For example, both intramolecular Cs···Cs distances in **16** are equal to 10.773(2) Å. In the case of **17**, these values change to 10.7647(8) and 10.8019(8) Å. To our surprise, much stronger distortions have been found in the supramolecular organizations of these compounds. Complex **16** forms a "stitch"-like 2D coordination polymer analogous to those discussed above for potassium- (**9**) and rubidium-based (**13–14**) compounds. The Cs···Ph half sandwich contacts supported by the coordination of each cesium ion by two ethanol solvates act as linking units. In turn, complex **17** represents an intriguing type of a 2D extended structure (Fig. 9, bottom). First of all, the cages in **17** are connected *via* Cs···Ph contacts and different types of Cs···O contacts. Two cesium ions are coordinated by two ethanol linkers, while two other ones are coordinated only by one ethanol linker. The corresponding intercage Cs···Cs contacts are equal to 4.493(3) and 5.4779(9) Å, respectively. Furthermore, one could see that (in the flat layer projection) the first and the fourth cages in the upper chain are not connected to the ones from the lower chain. This is due to the complicated "long stitch" style of the extended structure realized in **17**. Fig. 10 shows differences in the growth of the coordination polymer in two perpendicular directions from one cage chosen as the starting one. One could see that the central cage is on the crest of the wave position in the upper fragment and in the intermediate position in the lower fragment. It is interesting to compare it with the symmetrical style of "stitch" coordination polymer shown in Fig. 7. Due to such a "imbalance" in the central cage position, the 2D packing structure of **17** adopts other periodicity than that in compounds **9**, **13–14**, and **16**. Both wave fragments shown in Fig. 9 are longer than the periodic subunits of the stitch structure (Fig. 7) giving rise to another, "long stitch", style of packing observed in the case of **17**.

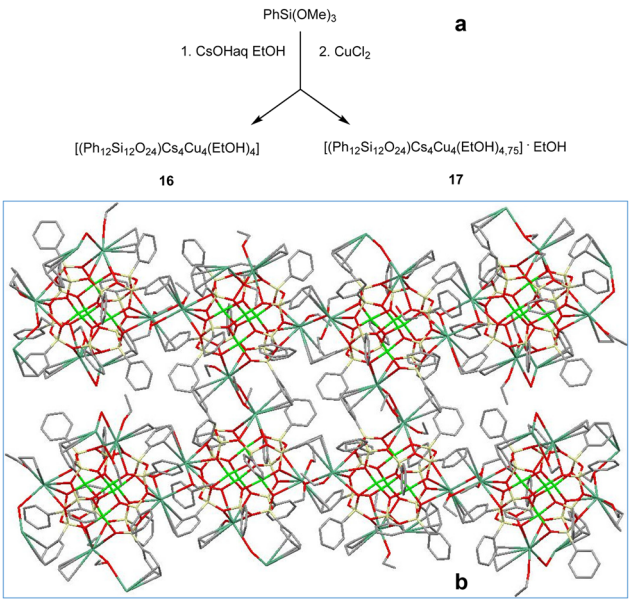

Fig. 9 (a) A general method for the synthesis of Cu_4Cs_4-phenylsilsesquioxanes **16 and 17**. (b) Simplified (flat layer) representation of the 2D "long stitch" supramolecular structure of **17**. Color code is the same as for Fig. 1, but with dark green Cs.

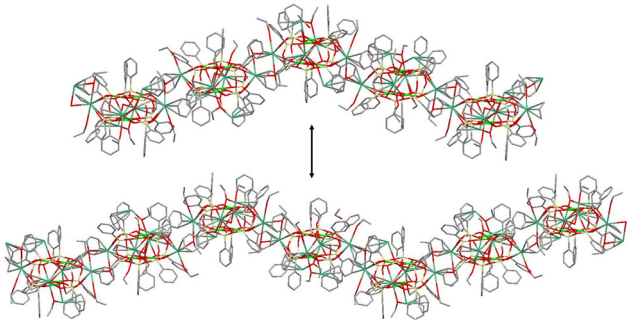

Fig. 10 Two wave-like 1D coordination polymer chains forming the 2D "long stitch" structure in **17**. Central (shared by both waves) cage is shown by an arrow. Bottom chain is rotated by 90° with respect to upper one for clarity.

Catalytic studies

Oxidation of alkanes. Complex **12**, chosen as a representative example, has been studied as a precatalyst in the oxidation of saturated hydrocarbons (Fig. 11 and S7–S11†). The oxidation of cyclohexane with hydrogen peroxide, according to gas chromatography, results in the formation of a mixture of cyclohexanol and cyclohexanone. The ratio of cyclohexanone to cyclohexanol is about 1.2 (0.033 M/0.026 M after 60 min). At the same time, the addition of triphenylphosphine to the reaction mixture according to the method proposed previously by Shul'pin[27] gives a much higher concentration of cyclohexanol and a sharp decrease in the amount of cyclohexanone, as shown in Fig. 11. The ratio of cyclohexanone to cyclohexanol after adding triphenylphosphine is about 0.07 (0.008 M/0.120 M after 60 min). The effect of adding triphenylphosphine to the reaction mixture can be explained by the fact that alkyl hydroperoxide is the main product of the oxidation reaction. In the absence of phosphine, it decomposes to form the respective ketone and alcohol in approximately equal amounts. Triphenylphosphine reduces all the alkyl hydroperoxide to alcohol, so one could see a sharp increase in the amount of alcohol on the chromatogram (see Fig. 11B). In many cases, the sum of alcohol and ketone before the addition of triphenylphosphine is much less than that after the addition of PPh_3. For example, the sum of ketone and alcohol amounts after 60 minutes is 0.06 M before the addition but

 This journal is © The Royal Society of Chemistry 2024

Published on 03 2024. Downloaded on 14.08.25 19:54:21.

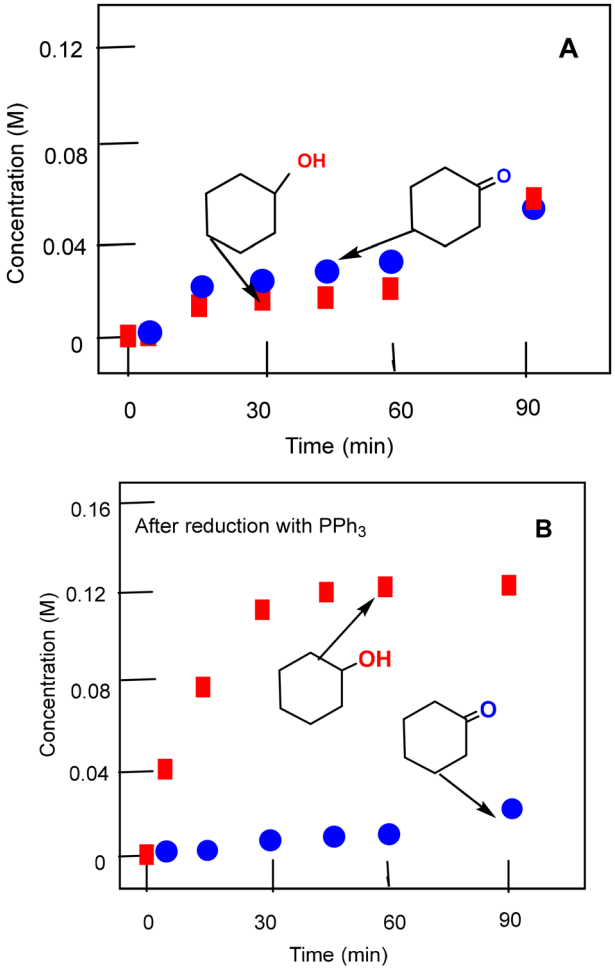

Fig. 11 Accumulation of cyclohexanol and cyclohexanone in the course of the oxidation of cyclohexane (0.46 M, 0.125 ml) with hydrogen peroxide (2.0 M, 50% aqueous, 0.32 ml) catalyzed by compound **12** (1×10^{-3} M, 5.2 mg) in the presence of HNO_3 (0.02 M, 0.02 ml of the stock solution of 65% aqueous HNO_3 in MeCN) in MeCN (up to 2.5 ml) at 60 °C. Concentrations of cyclohexanone and cyclohexanol were determined before adding PPh_3 (graph A) and after the reduction of the aliquots with solid PPh3 (graph B).

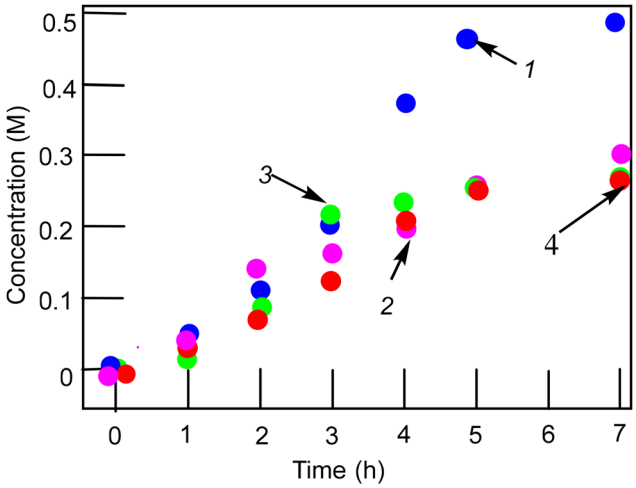

Fig. 12 Accumulation of acetophenone (curve 1, blue, yield 96%, TON = 960, TOF = 61), cyclohexanone (curve 2, pink, yield 57%, TON = 290, TOF = 41), 2-heptanone (curve 3, green, yield 50%, TON = 250, TOF = 36) and 2-hexanone (curve 4, red, yield 47%, TON = 240, TOF = 34) in the oxidation of 1-phenylethanol (0.5 M, 0.16 ml), cyclohexanol (0.5 M, 0.12 ml), 2-heptanol (0.5 M, 0.14 ml) and 2-hexanol (0.5 M, 0.12 ml) respectively, with *tert*-butyl hydroperoxide (1.5 M, 0.36 ml, 70% aqueous solution) catalysed by complex **12** (1×10^{-3} M) in the presence of HNO_3 (0.02 M) at 60 °C in acetonitrile.

increases to 0.128 M after the addition of PPh_3. The total yield of alcohol and ketone in the oxidation of cyclohexane for a 1-hour reaction is 28%, and TON is 129. To enable the oxidation of alkanes, nitric acid must be added to the reaction mixture. When carrying out reactions in the absence of nitric acid, only the decomposition of hydrogen peroxide (catalase activity) occurred, and the yield of the oxidation reaction products was about 1.4% in 120 minutes (Table S1†).

We also determined the selectivity parameters for the oxidation of certain alkanes (*n*-heptane and methylcyclohexane) by hydrogen peroxide catalyzed by complex **12**. For *n*-heptane, after two hours, the following concentrations (M) of alcohol isomers were obtained (after reduction with triphenylphosphine): C (1) 0.003 M; C (2) 0.007 M; C (3) 0.008 M; C (4) 0.004 M (yield 7%). These values gave a series of selectivity values: C (1) : C (2) : C (3) : C (4) = 1.0 : 4.4 : 4.4 : 5.0. In the case of methylcyclohexane oxidation, the following selectivity parameters were obtained: 1° : 2° : 3° = 1.0 : 5.4 : 14.8 (yield 15%). The selectivity parameters measured in the oxidation alkanes are close to the parameters typical for the reactions of alkanes with hydroxyl radicals.[28] Based on the experimental dependences of the reaction rates on the concentration of the reagents and using previously obtained data for the oxidation reactions with different metallocomplexes,[28,29] we can assume that the oxidation reactions of alkanes take place with the participation of hydroxyl species and alkyl hydroperoxides are formed as the main primary products.

Oxidation of alcohols. Complex **12** has also been successfully evaluated in the oxidation of different alcohols with *tert*-butyl hydroperoxide (Fig. 12). In order to quench the oxidation process, the concentrations of products were measured by GC after the reduction of the reaction samples with solid PPh_3. Values of yields, TONs and TOFs are given in the footnote to Fig. 12.

Conclusions

An impressive number (19 distinct compounds) of cage metallosilisesquioxanes have been synthesized using copper(II) ions as core centers and alkali metal ions as peripheral ones. The disposition of alkaline metal cations is mainly determined by their size. First, small lithium cations in **1** coordinate only two oxygen atoms of the siloxanolate ligand and are arranged linearly to the copper cations. Contrarily, large potassium (**9–12**), rubidium (**13**, **13a**, **14**, **15**) and cesium (**16**, **17**) cations are arranged in an arcuate manner to the copper cations, binding four oxygen atoms of the siloxanolate ligand. The sodium

Published on 03 2024. Downloaded on 14.08.25 19:54:21.

cations can also coordinate four oxygen atoms of the siloxanolate ligand; however, their disposition depends on both the cationic size and the different steric factors, for example, the steric volume of the coordinated solvent molecules. As a result, in the investigated cage-like Cu_4Na_4-based phenylsilsesquioxanes, sodium cations can arrange by all three types: (a) only linearly to the copper cations (**4**), (b) only arcuately to the copper cations (**3**, **6**, **6a**), and (c) both linearly and arcuately to the copper cations (**2**, **5**, **7**, **8**). The molecular structures of all 19 compounds are similar, representing the Cu_4M_4 nuclearity supported by a Si_{12}-based ligand. In turn, the compounds strongly differ from each other in their disposition to form coordination polymers. While the small size of lithium ions predictably resulted in island-like Cu_4Li_4 molecular structures, sodium-containing compounds could form 1D coordination polymers in the case of solvate species with low steric hindrances (*i.e.*, water) interlinking neighboring Cu_4Na_4 cages. In turn, Cu_4K_4 is capable of forming 0D, 1D, or 2D structures depending on the specific screening characteristics of the solvates. Cu_4Rb_4 and Cu_4Cs_4 compounds inevitably form extended (2D) structures. Packing trends of all described 2D coordination polymers (with K, Rb, or Cs ions) are different; along with classical 2D net organization, nontrivial "stitch" structures of interpenetrating waves are also available. Significant amounts of compounds have been isolated using acetone as a key solvating ligand. This supports our recent observations of the high efficiency of acetone surrounding the self-assembly of CLMSs.[20,21,30] A representative acetone-solvated Cu_4K_4-complex revealed a high catalytic activity in the peroxide oxidations of alkanes and alcohols. A strong influence of the nature of peroxide (H_2O_2 *vs.* TBHP) on catalytic activities towards different types of substrates has been noted. Keeping in mind the evidence that polynuclear compounds are often more active than copper mononuclear derivatives,[19a,23–26,31] further design of copper-based CLMSs, including coordination polymers, is of significant interest, and these investigations are currently ongoing in our team.

The data supporting this article have been included as part of the ESI.†

Crystallographic data for the article have been deposited at the CCDC under 2355320 (**1**), 2355321 (**2**), 2355322 (**3**), 2355323 (**4**), 2355324 (**5**), 2355325 (**6**), 2355326 (**6a**), 2355327 (**7**), 2355328 (**8**), 2355329 (**9**), 2355330 (**10**), 2355331 (**11**), 2355332 (**12**), 2355333 (**13**), 2355334 (**13a**), 2355335 (**14**), 2355336 (**15**), 2355337 (**16**), and 2355338 (**17**) and can be obtained from **https://www.ccdc.cam.ac.uk**.†

Conflicts of interest

There are no conflicts to declare.

Acknowledgements

We are grateful for the financial support from the Russian Science Foundation (RSF grant 22-13-00250, synthesis and catalytic studies). This work (elemental analysis) was in part supported by the Ministry of Science and Higher Education of the Russian Federation (Contract No. 075-03-2023-642) and was performed employing the equipment at the Center for Molecular Composition Studies of INEOS RAS.

References

1 (*a*) R. Murugavel, A. Voigt, M. G. Walawalkar and H. W. Roesky, *Chem. Rev.*, 1996, **96**, 2205; (*b*) V. Lorenz, A. Fischer, S. Gießmann, J. W. Gilje, Y. Gun'ko, K. Jacob and F. T. Edelmann, *Coord. Chem. Rev.*, 2000, **206–207**, 321; (*c*) R. W. J. M. Hanssen, R. A. van Santen and H. C. L. Abbenhuis, *Eur. J. Inorg. Chem.*, 2004, 675; (*d*) H. W. Roesky, G. Anantharaman, V. Chandrasekhar, V. Jancik and S. Singh, *Chem. – Eur. J.*, 2004, **10**, 4106; (*e*) V. Lorenz and F. T. Edelmann, *Adv. Organomet. Chem.*, 2005, **53**, 101; (*f*) M. M. Levitsky, B. G. Zavin and A. N. Bilyachenko, *Russ. Chem. Rev.*, 2007, **76**, 847; (*g*) F. T. Edelmann, in *Silicon Chemistry: From the Atom to Extended Systems*, ed. P. Jutzi and U. Schubert, Wiley, Darmstadt, Germany, 2003, pp. 383–394; (*h*) M. M. Levitsky and A. N. Bilyachenko, *Coord. Chem. Rev.*, 2016, **306**, 235; (*i*) Y. Zheng, Z. Gao and J. Han, *Curr. Org. Chem.*, 2018, **21**, 2814; (*j*) J. Ouyang, S. Haotian, Y. Liang, A. Commisso, D. Li, R. Xu and D. Yu, *Curr. Org. Chem.*, 2018, **21**, 2829; (*k*) M. M. Levitsky, Y. V. Zubavichus, A. A. Korlyukov, V. N. Khrustalev, E. S. Shubina and A. N. Bilyachenko, *J. Cluster Sci.*, 2019, **30**, 1283.

2 (*a*) M. M. Levitsky, A. N. Bilyachenko, E. S. Shubina, J. Long, Y. Guari and J. Larionova, *Coord. Chem. Rev.*, 2019, **398**, 213015; (*b*) K. Sheng, R. Wang, A. N. Bilyachenko, V. N. Khrustalev, M. Jagodič, Z. Jagličić, Z. Li, L. Wang, C. Tung and D. Sun, *ChemPhysMater*, 2022, **1**, 247; (*c*) K. Sheng, R. Wang, X. Tang, M. Jagodič, Z. Jagličić, L. Pang, J.-M. Dou, Z.-Y. Gao, Z.-Y. Gao, H.-Y. Feng, C.-H. Tung and D. Sun, *Inorg. Chem.*, 2021, **60**, 14866; (*d*) M. Tricoire, N. Jori, F. F. Tirani, R. Scopelliti, I. Zivkovic, L. S. Natrajan and M. Mazzanti, *Chem. Commun.*, 2024, **60**, 55.

3 (*a*) A. N. Kulakova, A. N. Bilyachenko, A. A. Korlyukov, J. Long, M. M. Levitsky, E. S. Shubina, Y. Guari and J. Larionova, *Dalton Trans.*, 2018, **47**, 6893; (*b*) A. N. Kulakova, A. N. Bilyachenko, A. A. Korlyukov, M. M. Levitsky, J. Long, Y. Guari and J. Larionova, *J. Organomet. Chem.*, 2021, **942**, 121815.

4 (*a*) Y.-N. Liu, J.-L. Hou, Z. Wang, R. K. Gupta, Z. Jagličić, M. Jagodič, W.-G. Wang, C.-H. Tung and D. Sun, *Inorg. Chem.*, 2020, **59**, 5683; (*b*) A. N. Kulakova, K. Nigoghossian, G. Félix, V. N. Khrustalev, E. S. Shubina, J. Long, Y. Guari, L. D. Carlos, A. N. Bilyachenko and J. Larionova, *Eur. J. Inorg. Chem.*, 2021, 2696; (*c*) G. Félix, S. Sene, A. N. Kulakova, A. N. Bilyachenko, V. N. Khrustalev, E. S. Shubina, Y. Guari and J. Larionova, *RSC Adv.*, 2023, **13**, 26302.

 This journal is © The Royal Society of Chemistry 2024

Published on 03 2024. Downloaded on 14.08.25 19:54:21.

5 (*a*) K. Sheng, Y.-N. Liu, R. K. Gupta, M. Kurmoo and D. Sun, *Sci. China, Ser. B: Chem.*, 2020, **64**, 419; (*b*) A. N. Kulakova, A. N. Bilyachenko, M. M. Levitsky, V. N. Khrustalev, E. S. Shubina, G. Felix, E. Mamontova, J. Long, Y. Guari and J. Larionova, *Chem. – Eur. J.*, 2020, **26**, 16594.

6 S. Marchesi, C. Bisio and F. Carniato, *Processes*, 2022, **10**, 758.

7 (*a*) K. Nigoghossian, A. N. Kulakova, G. Félix, V. N. Khrustalev, E. S. Shubina, J. Long, Y. Guari, S. Sene, L. D. Carlos, A. N. Bilyachenko and J. Larionova, *RSC Adv.*, 2021, **11**, 34735; (*b*) G. Félix, A. N. Kulakova, S. Sene, C. Charlot, A. N. Bilyachenko, A. A. Korlyukov, A. D. Volodin, E. S. Shubina, I. G. Elizbarian, Y. Guari and J. Larionova, *Organometallics*, 2023, **42**, 2613; (*c*) G. Félix, A. N. Kulakova, S. Sene, V. N. Khrustalev, M. A. Hernández-Rodríguez, E. S. Shubina, T. Pelluau, L. D. Carlos, Y. Guari, A. N. Carneiro Neto, A. N. Bilyachenko and J. Larionova, *Front. Chem.*, 2024, **12**, 1379587.

8 K. Sheng, W.-D. Si, R. Wang, W.-Z. Wang, J. Dou, Z.-Y. Gao, L.-K. Wang, C.-H. Tung and D. Sun, *Chem. Mater.*, 2022, **34**, 4186.

9 L. Qiao, W. Zhang and R. Yang, *Eur. Polym. J.*, 2024, **211**, 113027.

10 (*a*) X. Lin, Y. Dong, X. Chen, H. Liu, Z. Liu, T. Xing, A. Li and H. Song, *J. Mater. Chem. A*, 2021, **9**, 6423; (*b*) X. Lin, Y. Dong, X. Liu, X. Chen, A. Li and H. Song, *Chem. Eng. J.*, 2021, **428**, 132125.

11 (*a*) H. Chun and D. Moon, *J. Am. Chem. Soc.*, 2023, **145**, 18598; (*b*) A. N. Kulakova, A. N. Bilyachenko, A. A. Korlyukov, L. S. Shul'pina, X. Bantreil, F. Lamaty, E. S. Shubina, M. M. Levitsky, N. S. Ikonnikov and G. B. Shul'pin, *Dalton Trans.*, 2018, **47**, 15666; (*c*) A. N. Bilyachenko, G. S. Astakhov, A. N. Kulakova, A. A. Korlyukov, Y. V. Zubavichus, P. V. Dorovatovskii, L. S. Shul'pina, E. S. Shubina, N. S. Ikonnikov, M. V. Kirillova, A. Y. Zueva, A. M. Kirillov and G. B. Shul'pin, *Cryst. Growth Des.*, 2022, **22**, 2146; (*d*) A. N. Bilyachenko, I. S. Arteev, V. N. Khrustalev, L. S. Shul'pina, A. A. Korlyukov, N. S. Ikonnikov, E. S. Shubina, Y. N. Kozlov, N. Reis Conceição, M. F. C. Guedes da Silva, K. T. Mahmudov and A. J. L. Pombeiro, *Inorg. Chem.*, 2023, **62**, 13573; (*e*) G. S. Astakhov, M. M. Levitsky, A. A. Korlyukov, L. S. Shul'pina, E. S. Shubina, N. S. Ikonnikov, A. V. Vologzhanina, A. N. Bilyachenko, P. V. Dorovatovskii, Y. N. Kozlov and G. B. Shul'pin, *Catalysts*, 2019, **9**, 701.

12 (*a*) K. Wada and T.-A. Mitsudo, *Catal. Surv.*, 2006, **9**, 229; (*b*) P. Loganathan, R. S. Pillai, V. Jeevananthan, E. David, N. Palanisami, N. S. P. Bhuvanesh and S. Shanmugan, *New J. Chem.*, 2021, **45**, 20144.

13 A. N. Bilyachenko, E. I. Gutsul, V. N. Khrustalev, O. Chusova, P. V. Dorovatovskii, V. A. Aliyeva, A. B. Paninho, A. V. M. Nunes, K. T. Mahmudov, E. S. Shubina and A. J. L. Pombeiro, *Inorg. Chem.*, 2023, **62**, 15537.

14 (*a*) E. A. Quadrelli and J. M. Basset, *Coord. Chem. Rev.*, 2010, **254**, 707; (*b*) A. J. Ward, A. F. Masters and T. Maschmeyer, Metallasilsesquioxanes, in *Applications of Polyhedral Oligomeric Silsesquioxanes*, Springer, New York, NY, USA, 2011, vol. 3, pp. 135–166; (*c*) A. N. Bilyachenko, N. R. Conceição, M. F. C. G. da Silva, K. T. Mahmudov, G. B. Shul'pin and A. J. L. Pombeiro, in *Synthesis and Applications in Chemistry and Materials*, ed. A. J. L. Pombeiro, K. T. Mahmudov and M. F. C. G. da Silva, World Scientific, 2024. DOI: **10.1142/13309**; (*d*) G. S. Astakhov, V. N. Khrustalev, M. S. Dronova, E. I. Gutsul, A. A. Korlyukov, D. Gelman, Y. V. Zubavichus, D. A. Novichkov, A. L. Trigub, E. S. Shubina and A. N. Bilyachenko, *Inorg. Chem. Front.*, 2022, **9**, 4525; (*e*) M. M. Levitsky, A. I. Yalymov, A. N. Kulakova, A. A. Petrov and A. N. Bilyachenko, *J. Mol. Catal. A: Chem.*, 2017, **426**, 297.

15 G. S. Astakhov, M. M. Levitsky, X. Bantreil, F. Lamaty, V. N. Khrustalev, Y. V. Zubavichus, P. V. Dorovatovskii, E. S. Shubina and A. N. Bilyachenko, *J. Organomet. Chem.*, 2019, **906**, 121022.

16 S. Garg, D. K. Unruh and C. Krempner, *Catal. Sci. Technol.*, 2020, **11**, 211.

17 A. N. Bilyachenko, E. I. Gutsul, V. N. Khrustalev, P. V. Dorovatovskii, E. S. Shubina, E. S. Shubina, Y. Guari, G. Félix, J. Larionova, A. G. Mahmoud and A. J. L. Pombeiro, *Cryst. Growth Des.*, 2023, **23**, 8707.

18 P. Loganathan, R. S. Pillai, A. Jennifer, E. Varathan, M. Kesavan and S. Shanmugan, *New J. Chem.*, 2023, **47**, 8439.

19 (*a*) G. B. Shul'pin and L. S. Shul'pina, *Catalysts*, 2021, **11**, 186; (*b*) M. M. Levitsky, A. N. Bilyachenko and G. B. Shul'pin, *J. Organomet. Chem.*, 2017, **849–850**, 201; (*c*) A. N. Kulakova, A. N. Bilyachenko, V. N. Khrustalev, Y. V. Zubavichus, P. V. Dorovatovskii, L. S. Shul'pina, X. Bantreil, F. Lamaty, E. S. Shubina, M. M. Levitsky and G. B. Shul'pin, *Catalysts*, 2018, **8**, 484; (*d*) A. N. Bilyachenko, V. N. Khrustalev, P. V. Dorovatovskii, L. S. Shul'pina, N. S. Ikonnikov, E. S. Shubina, N. N. Lobanov, V. A. Aliyeva, A. V. M. Nunes, K. T. Mahmudov, Y. N. Kozlov and A. J. L. Pombeiro, *Inorg. Chem.*, 2024, **63**, 1909; (*e*) A. N. Bilyachenko, V. N. Khrustalev, G. S. Astakhov, A. Y. Zueva, I. S. Arteev, Y. V. Zubavichus, A. A. Korlyukov, P. V. Dorovatovskii, L. S. Shul'pina, N. S. Ikonnikov, M. V. Kirillova, E. S. Shubina, Y. N. Kozlov, A. M. Kirillov and G. B. Shul'pin, *Organometallics*, 2023, **42**, 2577.

20 A. N. Bilyachenko, V. N. Khrustalev, A. Y. Zueva, E. M. Titova, G. S. Astakhov, Y. V. Zubavichus, P. V. Dorovatovskii, A. A. Korlyukov, L. S. Shul'pina, E. S. Shubina, Y. N. Kozlov, N. S. Ikonnikov, D. Gelman and G. B. Shul'pin, *Molecules*, 2022, **27**, 6205.

21 A. N. Bilyachenko, I. S. Arteev, V. N. Khrustalev, A. Y. Zueva, L. S. Shul'pina, E. S. Shubina, N. S. Ikonnikov and G. B. Shul'pin, *Molecules*, 2023, **28**, 1211.

22 (*a*) N. Prigyai, S. Chanmungkalakul, V. Ervithayasuporn, N. Yodsin, S. Jungsuttiwong, N. Takeda, M. Unno,

Published on 03 2024. Downloaded on 14.08.25 19:54:21.

J. Boonmak and S. Kiatkamjornwong, *Inorg. Chem.*, 2019, **58**, 15110; (*b*) M. Laird, C. Totée, P. Gaveau, G. Silly, A. van der Lee, C. Carcel, M. Unno, J. M. Bartlett and M. Wong Chi Man, *Dalton Trans.*, 2021, **50**, 81.

23 A. N. Kulakova, A. A. Korlyukov, Y. V. Zubavichus, V. N. Khrustalev, X. Bantreil, L. S. Shul'pina, M. M. Levitsky, N. S. Ikonnikov, E. S. Shubina, F. Lamaty, A. N. Bilyachenko and G. B. Shul'pin, *J. Organomet. Chem.*, 2019, **884**, 17.

24 A. N. Kulakova, A. N. Bilyachenko, M. M. Levitsky, V. N. Khrustalev, A. A. Korlyukov, Y. V. Zubavichus, P. V. Dorovatovskii, F. Lamaty, X. Bantreil, B. Villemejeanne, J. Martinez, L. S. Shul'pina, E. S. Shubina, E. I. Gutsul, I. A. Mikhailov, N. S. Ikonnikov, U. S. Tsareva and G. B. Shul'pin, *Inorg. Chem.*, 2017, **56**, 15026.

25 A. N. Kulakova, E. E. Sedykh, M. M. Levitsky, P. V. Dorovatovskii, V. N. Khrustalev, L. S. Shul'pina, E. S. Shubina, Y. N. Kozlov, N. S. Ikonnikov, A. N. Bilyachenko and G. B. Shul'pin, *J. Organomet. Chem.*, 2019, **899**, 120911.

26 A. N. Bilyachenko, V. N. Khrustalev, A. Y. Zueva, E. M. Titova, G. S. Astakhov, Y. V. Zubavichus, P. V. Dorovatovskii, A. A. Korlyukov, L. S. Shul'pina, E. S. Shubina, Y. N. Kozlov, N. S. Ikonnikov, D. Gelman and G. B. Shul'pin, *Molecules*, 2022, **27**, 6205.

27 (*a*) G. B. Shul'pin, *J. Mol. Catal. A: Chem.*, 2002, **189**, 39; (*b*) G. B. Shul'pin, Y. N. Kozlov, L. S. Shul'pina and P. V. Petrovskiy, *Appl. Organomet. Chem.*, 2010, **24**, 464.

28 (*a*) A. E. Shilov and G. B. Shul'pin, *Activation and Catalytic Reactions of Saturated Hydrocarbons in the Presence of Metal Complexes*, Kluwer Academic Publishers, New York, NY, USA; Boston, MA, USA; Dordrecht, The Netherlands; London, UK; Moscow, Russia, 2002; (*b*) D. S. Nesterov, E. N. Chygorin, V. N. Kokozay, V. V. Bon, R. Boca, Y. N. Kozlov, L. S. Shul'pina, J. Jezierska, A. Ozarowski, A. J. L. Pombeiro and G. B. Shul'pin, *Inorg. Chem.*, 2012, **51**, 9110; (*c*) G. B. Shul'pin, D. S. Nesterov, L. S. Shul'pina and A. J. L. Pombeiro, *Inorg. Chim. Acta*, 2017, **455**, 666.

29 (*a*) M. Nandi and P. Roy, *Indian Chem. Eng., Sect. A*, 2013, **52**, 1263; (*b*) A. N. Bilyachenko, M. M. Levitsky, A. I. Yalymov, A. A. Korlyukov, A. V. Vologzhanina, Y. N. Kozlov, L. S. Shul'pina, D. S. Nesterov, A. J. L. Pombeiro, F. Lamaty, X. Bantreil, A. Fetre, D. Liu, J. Martinez, J. Long, J. Larionova, Y. Guari, A. L. Trigub, Y. V. Zubavichus, I. E. Golub, O. A. Filippov, E. S. Shubina and G. B. Shul'pin, *RSC Adv.*, 2016, **6**, 48165; (*c*) Y. N. Kozlov, G. V. Nizova and G. B. Shul'pin, *Russ. J. Phys. Chem.*, 2004, **78**, 184.

30 A. N. Bilyachenko, E. I. Gutsul, V. N. Khrustalev, G. S. Astakhov, A. Y. Zueva, Y. V. Zubavichus, M. V. Kirillova, L. S. Shul'pina, N. S. Ikonnikov, P. V. Dorovatovskii, E. S. Shubina, A. M. Kirillov and G. B. Shul'pin, *Inorg. Chem.*, 2022, **61**, 14800.

31 (*a*) I. S. Fomenko, M. Afewerki, M. I. Gongola, E. S. Vasilyev, L. S. Shul'pina, N. S. Ikonnikov, G. B. Shul'pin, D. G. Samsonenko, V. V. Yanshole, V. A. Nadolinny, A. N. Lavrov, A. V. Tkachev and A. L. Gushchin, *Molecules*, 2022, **27**, 4072; (*b*) Y. P. Petrenko, K. Piasta, D. M. Khomenko, R. O. Doroshchuk, S. Shova, G. Novitchi, Y. Toporivska, E. Gumienna-Kontecka, L. M. D. R. S. Martins and R. D. Lampeka, *RSC Adv.*, 2021, **11**, 23442; (*c*) A. Y. Zueva, A. N. Bilyachenko, I. S. Arteev, V. N. Khrustalev, P. V. Dorovatovskii, L. S. Shul'pina, N. S. Ikonnikov, E. I. Gutsul, K. G. Rahimov, E. S. Shubina, N. Reis Conceição, K. T. Mahmudov, M. F. C. Guedes da Silva and A. J. L. Pombeiro, *Chem. – Eur. J.*, 2024, e202401164; (*d*) I. S. Fomenko, O. S. Koshcheeva, N. I. Kuznetsova, T. V. Larina, M. I. Gongola, M. Afewerki, P. A. Abramov, A. S. Novikov and A. L. Gushchin, *Catalysts*, 2023, **13**, 849; (*e*) A. N. Bilyachenko, V. N. Khrustalev, E. I. Gutsul, A. Y. Zueva, A. A. Korlyukov, L. S. Shul'pina, N. S. Ikonnikov, P. V. Dorovatovskii, D. Gelman, E. S. Shubina and G. B. Shul'pin, *Molecules*, 2022, **27**, 8505.

 This journal is © The Royal Society of Chemistry 2024